Article:
Askew Page, HR, Dalsgaard, T, Baldwin, SN et al. (4 more authors) (2019) TMEM16A is implicated in the regulation of coronary flow and is altered in hypertension. British Journal of Pharmacology, 176 (11). pp. 1635-1648. ISSN 0007-1188

https://doi.org/10.1111/bph.14598

TMEM16A is Implicated in the Regulation of Coronary Flow and is Altered in Hypertension

Short title: TMEM16A in Coronary Arteries and Changes in Hypertension

HR Askew Page[1,2], T Dalsgaard[2], SN Baldwin [1], TA Jepps[2], Povstyan O[1], SP Olesen[2], IA Greenwood[1,2]

[1]Vascular Biology Research Centre, Institute of Molecular and Clinical Sciences, St George's University of London, London, SW17 0RE, UK.

[2]Department of Biomedical Sciences, Faculty of Health Sciences, University of Copenhagen, Blegdamsvej 3B, DK-2200 Copenhagen N, Denmark.

Word count of manuscript: 3369

Word count of abstract: 241

Acknowledgements

The authors would like to thank Professor Christian Aalkjær, University of Aarhus, for the use of the membrane potential recording equipment, and Dr Vincenzo Barrese, St. George's University of London, for his expert advice on the qPCR experiments.

Author Contributions

Askew Page designed and implemented all experiments, analysed data and drafted manuscript.

Dalsgaard, Baldwin, Jepps, and Povstyan undertook experiments and generated data.

SP Olesen was involved with funding provision.

Greenwood oversaw project, provided funding and construction of manuscript.

Corresponding author: grenwood@sgul.ac.uk

Abstract

Background and purpose: Coronary artery disease leads to ischaemic heart disease and ultimately myocardial infarction. Thus is it important to determine the factors that regulate coronary blood flow. Ca^{2+}-activated chloride channels contribute to the regulation of arterial tone; however, their role in coronary arteries is unknown. The aim of this study was to investigate the expression and function of the main molecular correlate of Ca^{2+}-activated chloride channels, TMEM16A, in rat coronary arteries.

Experimental approach: We performed mRNA and protein analysis, electrophysiological studies of coronary artery myocytes, and functional studies of coronary artery contractility and coronary perfusion, using novel inhibitors of TMEM16A. Furthermore, we assessed whether any changes in expression and function occurred in coronary arteries from spontaneously hypertensive rats.

Key Results: TMEM16A was expressed in rat coronary arteries. The TMEM16A-specific inhibitor, MONNA, hyperpolarised the membrane potential by -22.1mV in U46619, ($p=0.0017$). MONNA, $T16A_{inh}$-A01, and Ani9 attenuated 5HT/U46619-induced contractions, and MONNA and $T16A_{inh}$-A01 also increased coronary flow in Langendorff perfused rat heart preparations ($p=<0.0001$ for both drugs). TMEM16A mRNA was increased in coronary artery smooth muscle cells from spontaneously hypertensive rats (SHR), and U46619/5HT were more potent in arteries from SHRs (5HT EC_{50} in Wistars was 207±56 nM, versus 51±16 nM in SHRs, n=12 and n=13 respectively, $p<0.05$). MONNA diminished this increased sensitivity to U46619 and 5HT.

Conclusions and Implications: In conclusion TMEM16A is a key regulator of coronary blood flow and is implicated in altered contractility of coronary arteries from SHRs.

Abbreviations:

ACTA2	Actin alpha 2 smooth muscle
ANOVA	Analysis of Variance
ATP5B	ATP Synthase subunit Beta, mitochondrial
CaCC	Calcium-activated chloride channel
CADD	Combined annotation dependent depletion
CFTR	Cystic fibrosis transmembrane conductance regulator
CYC1	Cytochrome C1
GAPDH	Glyceraldehyde 3-phosphate dehydrogenase
GFP	Green fluorescent protein
I_{Cl}	Chloride current
I_{Cl}(Ca)	Calcium-activated chloride current
LAD	Left anterior descending (coronary artery)
LCPSS	Low chloride physiological saline solution
Myh11	Myosin Heavy Chain 11
Pecam1	Platelet and endothelial cell adhesion marker 1
PSS	Physiological saline solution
ROCK	Rho-associated protein kinase
SEM	Standard error of the mean
SHR	Spontaneously hypertensive rat
SNP	Single nucleotide polymorphism
Tnni3	Troponin I3
Tnnt2	Troponin T2

VGCC	Voltage-gated calcium channel
VSMC	Vascular smooth muscle cell
Vwf	Von Willebrand Factor
YWHAZ	14-3-3 protein zeta/delta
5HT	5 hydroxytryptamine

What is already known:

- TMEM16A proteins contribute to calcium-activated chloride channels.
- Reducing TMEM16A activity reduces vasoconstriction in pulmonary and mesenteric arteries.

What this study adds:

- TMEM16A blockers impaired vasoconstrictor responses in coronary artery and improved coronary blood flow.
- Coronary arteries from hypertensive rats exhibited raised TMEM16A and augmented vasoconstrictor sensitivity.

Clinical Significance:

- Targeting TMEM16A represents a new therapeutic target for ischaemic heart disease

CaCC - http://www.guidetopharmacology.org/GRAC/FamilyDisplayForward?familyId=130

U46619 - http://www.guidetopharmacology.org/GRAC/LigandDisplayForward?ligandId=1888

5HT - http://www.guidetopharmacology.org/GRAC/LigandDisplayForward?ligandId=5

VGCC - http://www.guidetopharmacology.org/GRAC/FamilyDisplayForward?familyId=80

Nicardipine - http://www.guidetopharmacology.org/GRAC/LigandDisplayForward?ligandId=2559

Caffeine - http://www.guidetopharmacology.org/GRAC/LigandDisplayForward?ligandId=407

CFTR - http://www.guidetopharmacology.org/GRAC/ObjectDisplayForward?objectId=707

Key words: Coronary, Smooth muscle, CaCC, TMEM16A, ANO1, chloride channels, blood flow, SHR, $T16_{inh}$-A01, MONNA.

Introduction

Coronary artery disease occurs when the narrowing of coronary arteries prevents sufficient cardiac perfusion. If left untreated, it can cause fatal myocardial infarctions. High blood pressure is a major risk factor for coronary artery disease, and reducing blood pressure is one of the best treatments to reduce or prevent coronary events. Cardiac perfusion is determined by flow through the coronary arteries, which is determined by the contractile state of the vascular smooth muscle cells as well as the presence of pathological impediments like atheroma or thrombi. Understanding what controls coronary artery smooth muscle contraction is necessary to comprehend what limits cardiac perfusion and to develop novel therapies.

TMEM16A (also known as ANO1) proteins contribute to the formation of chloride permeable channels that are activated by sub-micromolar concentrations of intracellular calcium (CaCCs). As vascular smooth muscle cells (VSMCs) actively accumulate chloride ions (Cl^-), activating CaCCs leads to Cl^- efflux and membrane depolarisation sufficient to activate VGCCs, and evoke contraction. Consequently, TMEM16A represents a possible factor in the development of vascular disease including hypertension and targeting these channels may be a viable new therapy. Whilst TMEM16A expression has been identified in several arteries (Dam et al., 2014; Davis et al., 2010; Manoury et al., 2010; Thomas-Gatewood et al., 2011) there is no data on TMEM16A in coronary arteries and whether it is altered in hypertension. Moreover, there is no information on the effect of recently developed TMEM16A-specific blockers in coronary arteries. The present study sought to address these points.

Methods

Animals: All experiments were performed on 1st and 2nd order branches of the left anterior descending coronary artery (LAD) and 1st order septal coronary arteries or 3rd order mesenteric arteries from male Wistar rats (aged 12-13 weeks, weighing 250-350g) (Charles River, Margate, UK) (RRID:RGD_737929), killed by cervical dislocation in accordance with schedule 1 of the UK Animal (Scientific Procedures) Act 1986. Spontaneously hypertensive rats (SHRs) (Envigo, UK) (RRID:RGD_724574) aged 12-13 weeks (weighing 250-300g) were used as an acknowledged model of essential hypertension. Rats were housed according to ASPA 1986 regulations with 12:12 hour light:dark cycle; 19-22 centigrade room temperature; room relative humidity within a range of 50% +/- 10%; received *ad*

libidum water (changed at least twice weekly) and laboratory rodent diet. Bedding was LBS Aspen Classic woodchip. Coronary arteries were identified and dissected free of the heart. The pericardium was peeled away from the surface of the heart and the right and left main coronary arteries were traced from the aortic root. Arteries were dissected free from myocardial tissue before they were used in any experiment. The LAD was identified as the main artery distal to the bifurcation at the left circumflex artery. The septal artery was identified by cutting away the right ventricular wall whence it could be seen running along the interventricular septum. The septal artery varied in its anatomical origin, sometimes arising from the right coronary artery and sometimes from the left.

Expression Studies: The expression of TMEM16A, as well as the reference genes ATP synthase subunit beta (ATP5B), cytochrome C1 (CYC1), 14-3-3 protein zeta/delta (YWHAZ), and glyceraldehyde 3-phosphate dehydrogenase (GAPDH) (predetermined by GeNorm (Biogazelle, Belgium) analysis) was measured by quantitative polymerase chain reaction (QPCR). The coronary artery SMC samples were obtained by cutting longitudinally along the dissected vessel and rubbing the lumen with a human hair. The vessel was then placed in 0.1% Triton X PBS for 1 minute followed by three 1 minute washes in fresh PBS to ensure removal of endothelium. The treated arteries were subsequently dispersed to a cell suspension as outline below before being spun down into a pellet and used for RNA extraction. Cardiac- and endothelial-cell specific primers were designed to check for contamination of the SMC sample. For a full list of primers used in this study see table 1. The primer sequences for housekeeping genes used for the GeNorm were unavailable due to proprietary reasons. QPCR samples were run in duplicate to

strengthen the reliability of the single value. Antibody AB53212 (AbCam, Cambridge, UK), used in previous studies (Pritchard et al., 2014) was used for immunochemical and Western blot studies (Abcam Cat# ab53212, RRID:AB_883075).

Functional studies. Wire myography was used to assess TMEM16A function in LAD coronary artery segments. Once the LAD coronary artery had been dissected free from surrounding cardiac tissue, segments were mounted onto the myograph (Danish MyoTech, Aarhus, Denmark) in PSS. The force on elicited by the tension of the vessel wall on the wires was recorded using LabChart software (ADInstruments, UK). For simultaneous membrane potential recordings, coronary artery segments were impaled with sharp glass microelectrodes with resistances of 60-130 MΩ, pulled on a horizontal puller (P-97 Sutter Instrument Co., USA), that were filled with 3M KCl. The reference electrode (flat-tip Ag/AgCl probe; Warner Instrument, USA) was submerged into the myograph chamber and the amplifier was zeroed with the recording electrode lowered into the bath solution. Voltage was recorded at 1 kHz through an amplifier (Intra 767, WPI Ltd.) and A-D converter (PowerLab 4SP, ADInstruments, New Zealand). Impalements were deemed suitable when there was an abrupt, negative deflection in potential which rapidly returned to the pre-impalement level upon withdrawal from the cell. In both settings the vessel segments were bathed in PSS (in mM: NaCl 119, KCl 4.5, $MgSO_4 \cdot 7H_2O$ 1.17, $NaH_2PO_4 \cdot 2H_2O$ 1.18, $NaHCO_3$ 25, Glucose 5, $CaCl_2$ 1.25), heated to 37°C and aerated with 95% O_2, 5% CO_2.

For Langendorff studies, hearts were swiftly dissected and the ascending aorta was tied onto a perfusion cannula attached to a vertical perfusion rig (Hugo Sachs Elektronik-Harvard Apparatus GmbH, Germany). This allowed retrograde perfusion

of the heart. The heart was perfused at 80 mmHg with Krebs-Henseleit solution (in mM: 118 NaCl, 4.7 KCl, 2 $CaCl_2$, 1.2 KH_2PO_4, 1.2 Mg_2SO_4, 2 Sodium Pyruvate, 24.9 $NaHCO_3$, and 10 glucose, pH 7.45, aerated with 95% O_2, 5% CO_2), heated to 37°C, and filtered through an in-line 0.45 μm Sterivex HV filter (Millipore A/S, Hellerup, Denmark). Coronary flow was measured using an ultrasonic flow meter probe (Transonic Systems Inc., Ithaca, USA) situated above the aortic cannula. Aortic pressure, coronary flow, ECG, and perfusate temperature were continuously monitored. Coronary flow was measured using a 16-channel PowerLab system (ADInstruments, Oxford, UK) and recorded by LabChart 7 software. The heart was left until the basal coronary flow had stabilised before any drugs were added to the perfusate.

Single cell electrophysiology. Single smooth muscle cells were isolated from LAD coronary arteries by enzymatic treatment. The dissected vessel was placed into ice cold, Ca^{2+}-free dispersal PSS (in mM: NaCl 120, KCl 6, Glucose 12, HEPES 10, $MgCl_2$ 1.2, pH adjusted to 7.4 with NaOH). The solution was then supplemented with 1.75 mg/ml Collagenase IA, 0.9 mg/ml Protease X, 1 mg/ml BSA, and 1 mg/ml Trypsin inhibitor and incubated at 37°C for 9 minutes. Following this, the vessels was washed with ice cold dispersal PSS 3 times. After the last wash, the tube was filled with 1 mL of dispersal PSS and the vessel was triturated with a fire-polished, wide-bore Pasteur pipette to liberate the VSMCs mechanically. The resultant cell suspension was then supplemented with $CaCl_2$ to 0.75mM and plated onto coverslips before being left to settle at 4°C before use.

Whole cell currents were recorded following amphotericin B permeabilization (300 μg/ml) in the absence and presence of 10 mM caffeine. Amphotericin was added to

the pipette solution (in mM: CsCl 106, TEA-Cl 20, HEPES 10, EGTA 10, pH adjusted to 7.2 with CsOH), which was refreshed every two hours for consistent Amphotericin activity. The cells were superfused with bathing solution (in mM: NaCl 120, TEA-Cl 5, KCl 6, glucose 12, HEPES 10, $MgCl_2$ 1.2, $CaCl_2$ 1.5, pH adjusted to 7.4 with NaOH). Currents evoked by caffeine application were recorded during a ramp protocol which stepped to -100 mV from a -50 mV holding potential, and steadily increased to +100 mV over 2 seconds. MONNA was applied in the caffeine-free bathing solution before the protocol was repeated in the presence of both drugs. Where possible, drugs were applied while recording from the same cell as the initial caffeine application. Cells were always compared to same day controls. Similar experiments were performed on pulmonary artery cells where $I_{Cl(Ca)}$ has been characterised extensively (Manoury et al., 2010; Pritchard et al., 2014).

Statistical Analysis and Blinding: For all graphs the error bars represent standard error of the mean (SEM) of no less than 5 independent data points. Each data point represents data collected from one animal. Data from myography experiments are expressed as a percentage of the peak contraction in response to a maximal concentration of U46619 or 5HT, or the peak of the first high K^+-induced contraction/EC_{80}-induced contraction. This is to control for variation in the overall contractility of the vessel segment. Similarly, in the Langendorff experiments, data is expressed as percentage change in flow to control for varying heart sizes and therefore innate differences in coronary flow. Randomisation of samples was undertaken in the functional experiments by scrambling the vessel segments before mounting them into the myograph chambers. In this way vessel segments from higher or lower down the coronary artery branch were randomised to whether they

were subjected to treatment or control conditions. Blinding of the experiments was impractical due to the experimenter adding differing concentrations of drugs to the set-ups. Concentration effect curves were log transformed to reduce the skew and curves were fitted to the data using four-parameter, non-linear regression curve fitting in GraphPad Prism (version 7.0b) (GraphPad Prism, RRID:SCR_002798) with the following formula: Y=Bottom + (Top-Bottom)/(1+10^((LogEC50-X)*HillSlope)) where x is [agonist] (in log M), Y is the percentage of the peak contraction mentioned above, Top refers to F_{max} (maximal percentage), Bottom refers to F_{min} (average percentage contraction at lowest concentration of agonist), and the Hill Slope is variable. Comparisons of responses ± blocker vs same-day/animal controls were compared by two-way analysis of variance (ANOVA), followed by a *post hoc* test (Bonferonni) for multiple comparisons. Peak contraction studies ± inhibitor and ± Cl^- were compared to same day/animal controls using paired or unpaired Students two-tailed *t*-test where appropriate. Comparisons between Wistars and SHRs were made using data from earlier experiments in order to reduce animal numbers. Therefore data were not paired for analysis and the n numbers are not equal. Statistical significance is defined as $P<0.05$ (*). Two stars indicate $P\leq0.01$, three stars - $P\leq0.005$, four stars - $P\leq0.001$.

Reagents: All drugs and reagents were purchased from Sigma-Aldrich (Dorset, UK) unless otherwise stated. MONNA, T16Ainh-A01, and Ani9 (Tocris, UK) block Cl^- currents generated by the over-expression of TMEM16A, or endogenous TMEM16A currents with IC_{50}s of about 0.1, 1, and 0.1 µM, respectively (Namkung et al., 2011; Oh et al., 2013; Seo et al., 2016).

Nomenclature of Targets and Ligands

Key protein targets and ligands in this article are hyperlinked to corresponding entries in http://www.guidetopharmacology.org, the common portal for data from the IUPHAR/BPS Guide to PHARMACOLOGY (Harding et al., 2018), and are permanently archived in the Concise Guide to PHARMACOLOGY 2017/18 (Alexander et al., 2017).

Results

TMEM16A is Expressed in Rat Coronary Arteries:

Quantitative PCR revealed expression of TMEM16A, and extremely low expression of the close orthologue TMEM16B in LAD and septal coronary arteries (figure 1A). The relative level of TMEM16A expression was higher than mesenteric arteries but lower than pulmonary arteries (figure 1B) where CaCCs have been well characterised (Angermann et al., 2012; Davis et al., 2013; Greenwood et al., 2001; Greenwood et al., 2004; Manoury et al., 2010; Piper & Large, 2003; Piper & Greenwood, 2003; Pritchard et al., 2014; Wang et al., 1992; Wiwchar et al., 2009; Yuan, 1997). In Western blot studies (figure 1C), untransfected and GFP-tagged TMEM16A transfected HEK293 cells were used to further validate anti-TMEM16A antibody AB53212 for use in immunocytochemical/histochemical experiment. Rat pulmonary artery lysates were also used as the expression of TMEM16A has previously been characterised here (Pritchard et al., 2014; Sun et al., 2012). Antibody AB53212 produced a band close to the theoretical molecular weight for TMEM16A (~120 kDa) in lysates from rat pulmonary artery and the two HEK cell samples. A band was also detected around 145 kDa in lysates of HEK cells transfected with GFP-tagged TMEM16A. No band was detected at these molecular

weights from rat coronary artery (n=3 complete isolations, where each isolation consisted of 3 rats worth of arteries). The distribution of TMEM16A encoded protein was investigated in isolated coronary artery smooth muscle cells. Figure 1D shows representative images of TMEM16A staining. Imaging of cells incubated with the TMEM16A antibody AB53212 (figure 1D i-iv) showed disperse TMEM16A staining throughout the cytoplasm with more intense punctate regions both centrally and around the extremities of the cell (examples indicated by arrows 1 and 2). Expression of TMEM16A protein was also observed in transverse sections of coronary arteries *in situ* (fig 1E) delineated by α-smooth muscle actin staining (indicated by arrow 1 and 3). TMEM16A was also detected in the surrounding, troponin-positive myocardium.

These data show that TMEM16A is expressed in coronary artery SMCs.

TMEM16A Activation is Integral to Agonist-Induced Contraction of Rat Coronary Arteries

When LAD coronary artery segments were incubated in a low chloride physiological saline solution (LCPSS), contractions to both U46619 and 5HT were reduced considerably (figures A and B, respectively). Bathing LAD coronary artery segments in high K^+-PSS produced robust and reproducible contractions that were not affected by incubation with 10 μmol/L MONNA (figure 3C) suggesting the agent did not directly inhibit VGCCs. Application of U46619 and 5HT produced concentration-dependent contractions with approximate EC_{50} values of 37±7 nmol/L (n=27) and 207±56 nmol/L (n=12), respectively. These contractions were abolished by prior incubation with 10 nmol/L nicardipine (figure S1) indicating that activation of VGCCs was crucial for contractions brought about by both U46619 and 5HT. Application of

MONNA inhibited the contractile response to U46619 and 5HT in a concentration dependent manner (figures 3D and E, and F and G). The inhibitory effect of MONNA was not reliant upon a functional endothelium (figures 3I and J) and was not altered by incubation with a cocktail of K^+ channel blockers (figure H).

Effect of $T16A_{inh}$-A01 and Ani9 on Contraction of LAD Coronary Arteries

High K^+-induced contractions of LAD coronary artery segments were significantly inhibited by pre-incubation with 10 µmol/L $T16A_{inh}$-A01 (figure 3B). While 3 µmol/L $T16A_{inh}$-A01 and Ani9 did not cause statistically significant attenuations in the high K^+-induced contractions, there was a trend for high K^+-induced (figures 3B and A respectively). In further experiments, Ani9 caused a small, but significant attenuation in the U46619-induced contraction although, given the data in figure 3A, it is difficult to say whether this was due to TMEM16A inhibition (figure 3C). $T16A_{inh}$-A01 caused leftward shifts in the U46619 concentration-effect curves in LAD coronary artery segments at both 3 and 10 µmol/L (figures 3D and E). Interestingly, the effect of pre-incubation with 3 µmol/L $T16A_{inh}$-A01 was more marked that with 10 µmol/L $T16A_{inh}$-A01 and 3 µmol/L Ani9. 10 µmol/L $T16A_{inh}$-A01 also caused an inhibition of 5HT-induced contractions in LAD coronary arteries. This inhibition of U46619- and 5HT-induced contractions with 10 µmol/L $T16A_{inh}$-A01 was also seen in septal coronary arteries (figure S2). Given the data in figures 2 C-J where MONNA did not cause an effect on the high K^+-induced contractions, and its effect on agonist-induced contractions was independent of endothelium, and was unchanged in the present of a cocktail of potassium channel blockers, we decided to use MONNA for further studies.

Involvement of TMEM16A in coronary perfusion

The influence of TMEM16A channels on coronary blood flow in whole hearts was investigated using a Langendorff preparation. Application of either MONNA or $T16A_{inh}$-A01 (10 nmol/L – 1 µmol/L) enhanced coronary flow (figure 2A) without any effect on cardiac parameters. The QT and RR intervals recorded during these experiments can be seen in tables 2 and 3. MONNA (1 µmol/L) also prevented the decreased coronary flow produced by infusion of the thromboxane A_2 receptor agonist U46619 (10 nmol/L, figure 4B and C). These data show that pharmacologically disabling TMEM16A improves coronary blood flow.

MONNA Attenuates Caffeine-Evoked Chloride Currents in Coronary Artery VSMCs and Decreases Membrane Potential of U46619-Constricted Coronary Arteries

In line with previous studies investigating CaCCs (Greenwood et al., 2001), caffeine was used to mobilise Ca^{2+} from the sarcoplasmic reticulum and evoke $I_{Cl(Ca)}$. Reproducible caffeine-evoked chloride currents were recorded in LAD coronary artery VSMCs in the absence, but not in the presence of, 10 µmol/L MONNA (figure 5A). Caffeine produced considerably larger, faster inward currents in these cells at -50 mV (Fig 5A). Similar results were seen in experiments carried out on pulmonary artery smooth muscle cells (figure S3). In sharp microelectrode recordings on whole LAD coronary arteries application of an EC_{50} concentration of U46619 contracted arteries with an associated depolarisation of the membrane potential (Figure 5B). Application of 10 µmol/L MONNA caused membrane potential repolarisation (figure 5B). This change in membrane potential was accompanied by a simultaneous decrease in wall tension.

Altered Expression of TMEM16A in SHR Coronary Artery SMCs

SMCs were isolated from coronary arteries as described above. The cleanliness of the SMC preparation was confirmed by qPCR analysis of cardiac- and endothelial cell-specific markers (troponin T2 (Tnnt2), troponin I3 (Tnni3), Von Willebrand Factor (Vwf), and platelet and endothelial cell adhesion marker (Pecam). Tmem16a expression was greatest in the SMC sample and at low levels in ventricular tissue and endothelial cells. The SMC samples were highly positive for the smooth muscle markers alpha smooth muscle actin (Acta2), and myosin heavy chain 11(Myh11), while comparatively negligible levels of expression of the cardiac and endothelial cell-specific markers were found in the SMC sample. All data for these experiments can be found in the supplement (Figure S4). This established that the SMC sample was free from cardiac and endothelial contamination. QPCR analysis showed a ~four-fold increase in expression of TMEM16A in the coronary artery SMCs of SHRs when compared to Wistar controls (figure 6A). Importantly, TMEM16A expression in ventricular tissue, where protein staining can be seen (figure 1Eiii), was not increased in the ventricular tissue of SHRs (figure 6B). This finding adds further credence to the fact that the results seen in figure 6A are not due to any contribution from cardiac myocytes.

Altered Function of TMEM16A in SHR LAD Coronary Arteries

Functional experiments revealed that LAD segments had a greater sensitivity to U46619 and 5HT compared to segments from normotensive rats contracting more in response to lower concentrations without a change in the maximal contractile response (figure 7C and D respectively). 30 nmol/L 5HT caused a contraction of 0.12

± 0.05 mN in LAD coronary artery segments of Wistars while it caused a much bigger contraction of 1.23 ± 0.32 mN in those of SHRs (p=0.0018), equivalent to a ~10 fold increase in contraction. This increased sensitivity was abolished by application of 10 µmol/L MONNA (figure 7B). Similar effects were seen in the U46619 contraction study (figure 7A). In addition, LAD segments from SHRs exhibited a higher level of spontaneously-developed basal tone, which was abrogated by 10 µmol/L MONNA (figure 7I). In contrast, the overall contractility of LAD coronary artery segments from SHRs in response to U46619 and 5HT was less sensitive to inhibition by MONNA than in LAD coronary arteries from normotensive rats (figures 7E, F, G and H). This is reflected in the mean EC_{50} values highlighted in table 4. In summary, expression of TMEM16A mRNA is higher in coronary arteries from SHRs that was associated with a MONNA-sensitive increase in basal tone and responsiveness to low concentrations of U46619 and 5HT.

Discussion

This study is the first to identify expression of TMEM16A in coronary arteries and implicate it in determination of coronary perfusion. In addition, we report changes in TMEM16A expression and function in coronary arteries from hypertensive rats.

We show that MONNA, at concentrations that inhibit TMEM16A mediated Cl^- currents in over-expression systems, inhibited $I_{Cl(Ca)}$ in coronary artery myocytes, attenuated contractions produced by U46619 and 5HT, reversed membrane depolarisation produced by U46619, inhibited spontaneously induced basal tone and improved coronary blood flow. These anti-contractile effects were not dependent upon a functional endothelium, nor were they affected by incubation of the coronary artery with several K^+-channel blockers. Moreover, they did not reflect a direct block

of calcium channels as contractions produced by high K^+ solutions were not affected by MONNA, although two other TMEM16A blockers, $T16A_{inh}$-A01 and Ani9, did affect high K^+ spasms moderately. Incubation of the coronary arteries in low Cl^- bathing solution also attenuated 5HT- and U46619-induced contractions considerably. These consolidated data provide evidence that activation of TMEM16A-comprising Cl^- channels produces sufficient depolarisation to increase calcium channel opening and produce vasoconstriction in response to two different receptor agonists as well as at rest in certain conditions. By inference these data implicate TMEM16A channels as key determinants of coronary perfusion. However, Boedtkjer et al. (2015) have challenged the specificity of $T16A_{inh}$-A01, and to a lesser extent, that of MONNA. They reported no difference in contractions of rat mesenteric arteries to noradrenaline in the absence or presence of Cl^- in the PSS. Moreover, 10 μmol/L of both $T16A_{inh}$-A01 and MONNA inhibited the Cl^- independent contraction seen in the mesenteric arteries, indicating that these two inhibitors abrogate contractility of these vessels in the absence of a functional chloride gradient. Our data in coronary arteries concurs with their finding that $T16A_{inh}$-A01 relaxed rat mesenteric arteries contracted with a high extracellular K^+-containing (60 mmol/L) saline solution. This supports Boedtkjer et al.'s (2015) proposal that this agent inhibited vasospasm by means other than inhibiting $I_{Cl(Ca),}$ with direct blockade of calcium channels most likely. However, our data did not emulate the low Cl^- experiment findings of Boedtkjer et al. (2015) and we have no explanation for these differences. Our extensive characterisation of MONNA gave us no reason to doubt its specificity for TMEM16A. Nonetheless, it is curious that so many purportedly TMEM16A-specific inhibitors also cause a decrease in the high K^+-induced contraction. Interestingly, a reduction in high K^+-induced contraction and expression

of VGCCs has been reported upon TMEM16A knockdown in rat mesenteric arteries (Dam et al., 2014), and more recently, constitutive TMEM16A-targetted siRNA downregulation was associated with a concurrent decrease in L-type voltage-gated Ca^{2+} channel protein expression (Jensen et al., 2018). This questions whether $T16A_{inh}$-A01 and Ani9 are indeed blocking TMEM16A and causing a similar effect to that of TMEM16A knockdown. It could be possible that TMEM16A has a regulatory function that modulates other ion channels, as suggested in Jensen *et al.* (2018). CFTR, another Cl^- channel, negatively regulates CaCCs in bovine pulmonary arteries (Wei et al., 1999). Furthermore, it indicates that TMEM16A could be coupled to VSMC contraction in ways other than the direct depolarising effect of $I_{Cl(Ca)}$. Indeed a recent paper has implicated TMEM16A in the RhoA/ROCK signalling pathway (Li et al., 2016). This could possibly account for the results seen in the Cl^- free experiments in Boedtkjer et al. (2015) in which mesenteric arteries still produce TMEM16A-inhibitor sensitive noradrenaline-induced contractions.

We observed an increase of TMEM16A transcript in coronary and arteries from SHRs, which exhibited a greater level of spontaneous basal tone development. Furthermore, we show that U46619 and 5HT were more effective at eliciting contraction at lower concentrations (10 and 30 nmol/L respectively) in arteries from SHRs and these responses along with the heightened basal tone were abrogated by MONNA. Interestingly, our study shows that inhibition of TMEM16A was less effective against maximal contractions in arteries from SHRs compared to Wistar controls, similar to a previous report by Wang et al. (2015). These results suggest that the increase in contractility of coronary arteries from SHRs could be due to the increased expression of TMEM16A causing greater depolarisation and therefore Ca^{2+} influx. In support of this hypothesis, VSMC specific knockout of TMEM16A

reduced systemic blood pressure and attenuated the development of hypertension in mice (Heinze et al., 2014) and knockdown of TMEM16A with siRNA prevented the increase in systolic blood pressure in SHRs (Wang et al., 2015). Furthermore, pulmonary arteries from animals with monocrotaline- or chronic hypoxia-induced hypertension have increased TMEM16A protein and $I_{Cl(Ca)}$ density (Forrest et al., 2012; Sun et al., 2012). Ideally, we would like to show increased protein expression by Western blot in the coronary arteries of SHRs, similar to studies in other arteries of SHRs (Wang et al., 2015). However, we were not able to detect a band at ~120 kDa in lysates from coronary artery or mesenteric artery even though robust staining was detected in immunocytochemical studies with the validated anti-TMEM16A antibody, AB53212. These findings suggest that the molecular isoforms of TMEM16A may differ in different arteries with the pulmonary artery exhibiting the conventional full-length form. A truncated isoform of TMEM16A has been identified in the interstitial cells of Cajal of patients with diabetic gastroparesis (Mazzone et al., 2011) and future studies will focus on the relative abundance of these truncated variants over the full-length form in arterial regulation.

As inhibiting TMEM16A improved coronary perfusion then any upregulation in expression or activation efficiency would narrow coronary arteries, contributing to the development of coronary artery disease. Given the strong association between hypertension and coronary artery disease, we suggest that these findings have important implications in the pathogenesis of coronary artery disease and that targeting TMEM16A may not only prove an effective mechanism to reduce blood pressure but also increase coronary artery blood flow and cardiac perfusion. Interrogation of a UK Biobank database containing >400,000 individuals identified a

novel single nucleotide polymorphism in the coding region of the TMEM16A gene that is strongly associated with the pathogenesis of essential hypertension. We performed combined annotation dependent depletion (CADD) analysis of all 51 loci identified to be associated with essential hypertension in the UK Biobank and found that the SNP associated with TMEM16A (rs2186797) was the most deleterious of all SNPs associated with hypertension (see table in supplement). CADD prioritises functional, deleterious and pathogenic variants across many categories, and CADD scores of ≥20 are predictive of the 1% most deleterious substitutions to the human genome. This analysis of the large data set provided by the UK Biobank provides powerful support for TMEM16A in the pathogenesis of hypertension, that consolidates animal studies with TMEM16A deficient mice (Heinze et al., 2014) and the pharmacological or molecular disabling of TMEM16A. Importantly, the caveat must be made that the functional impact of the SNP in question on TMEM16A is not currently known. Future studies will investigate how this variant may change the structure and function of the TMEM16A protein so it is possible to hone in on what it is that leads to pathology. The future impact of this could be dramatic if the defect in TMEM16A can be rectified pharmacologically. Interestingly, it is not the first time this gene variant of TMEM16A has been reported in relation to a cardiovascular pathology. Shiffman et al. (2006) found that the allele frequency of the rs2186797 TMEM16A gene variant was significantly increased in patients with early-onset myocardial infarction (Shiffman et al., 2006) - an observation made pertinent by the findings of the present study. More recently, a different variant of TMEM16A, rs7127129, was identified as being associated with changes in the aortic root diameter of patients with heart failure (Wild et al., 2017). Recent investigations have resolved the atomic structure of murine TMEM16A transmembrane domains which

could facilitate identifying how these SNPs cause functional variation. Given the noteworthy CADD score of the rs2186797 variant (>21), the expressional and functional changes of TMEM16A in coronary arteries from SHRs outlined above, and the other reports of TMEM16A SNPs in cardiovascular disease, as well as previous reports of TMEM16A's role in animal models of hypertension, there is a plethora of evidence to suggest that irregularities in expression and function of TMEM16A contribute to cardiovascular pathology.

In conclusion, this study provides evidence for an important role of TMEM16A in rat coronary arteries under normal physiological circumstances, but also in the pathophysiology of hypertension. Future studies will help clarify the role of TMEM16A in the vasculature and in cardiovascular diseases, not only as an ion channel regulating $I_{Cl(Ca)}$, but also as a multifunctional protein, which may modulate the function of other ion channels. Furthermore, investigations of the functional impact of the SNP in the TMEM16A coding region could help to elucidate how this SNP contributes to the pathology of hypertension in humans.

Sources of Funding

TD was funded by Novo Nordsk Foundation (Grant number 6553). IAG received a Lundbeck Fellowship and receives funding from the British Heart Foundation and Medical Research Council (UK).

Conflict of Interest/Disclosures

None

Declaration of transparency and scientific rigour

This Declaration acknowledges that this paper adheres to the principles for transparent reporting and scientific rigour of preclinical research as stated in the *BJP* guidelines for Design & Analysis, Immunoblotting and Immunochemistry, and Animal Experimentation, and as recommended by funding agencies, publishers and other organisations engaged with supporting research.

References

Alexander, S. P., Kelly, E., Marrion, N. V, Peters, J. A., Faccenda, E., Harding, S. D., … CGTP Collaborators. (2017). THE CONCISE GUIDE TO PHARMACOLOGY 2017/18: Overview. *British Journal of Pharmacology*, *174*, S1–S16. http://doi.org/10.1111/bph.13882

Angermann, J. E., Forrest, A. S., Greenwood, I. A., & Leblanc, N. (2012). Activation of Ca2+-activated Cl- channels by store-operated Ca2+ entry in arterial smooth muscle cells does not require reverse-mode Na+/Ca2+ exchange. *Canadian Journal of Physiology and Pharmacology*, *90*(7), 903–21. http://doi.org/10.1139/y2012-081

Boedtkjer, D. M. B., Kim, S., Jensen, A. B., Matchkov, V. M., & Andersson, K. E. (2015). New selective inhibitors of calcium-activated chloride channels-T16Ainh -A01, CaCCinh -A01, and MONNA-what do they inhibit? *British Journal of Pharmacology*. http://doi.org/10.1111/bph.13201

Dam, V. S., Boedtkjer, D. M., Aalkjaer, C., & Matchkov, V. (2014). The bestrophin- and TMEM16A-associated Ca 2+ -activated Cl – channels in vascular smooth muscles. *Channels*, *8*(4), 361–369. http://doi.org/10.4161/chan.29531

Dam, V. S., Boedtkjer, D. M. B., Nyvad, J., Aalkjaer, C., & Matchkov, V. (2014). TMEM16A knockdown abrogates two different Ca(2+)-activated Cl (-) currents and contractility of smooth muscle in rat mesenteric small arteries. *Pflügers Archiv : European Journal of Physiology*, *466*(7), 1391–409. http://doi.org/10.1007/s00424-013-1382-1

Davis, A. J., Forrest, A. S., Jepps, T. A., Valencik, M. L., Wiwchar, M., Singer, C. A., … Leblanc, N. (2010). Expression profile and protein translation of TMEM16A in murine smooth muscle. *American Journal of Physiology. Cell Physiology*, *299*(5), C948-59. http://doi.org/10.1152/ajpcell.00018.2010

Davis, A. J., Shi, J., Pritchard, H. A. T., Chadha, P. S., Leblanc, N., Vasilikostas, G., … Greenwood, I. A. (2013). Potent vasorelaxant activity of the TMEM16A inhibitor T16A(inh) -A01. *British Journal of Pharmacology*, *168*(3), 773–84. http://doi.org/10.1111/j.1476-5381.2012.02199.x

Forrest, A. S., Joyce, T. C., Huebner, M. L., Ayon, R. J., Wiwchar, M., Joyce, J., … Leblanc, N. (2012). Increased TMEM16A-encoded calcium-activated chloride channel activity is associated with pulmonary hypertension. *American Journal of Physiology. Cell Physiology*, *303*(12), C1229-43. http://doi.org/10.1152/ajpcell.00044.2012

Greenwood, I. A., Ledoux, J., & Leblanc, N. (2001). Differential regulation of Ca(2+)-activated Cl(-) currents in rabbit arterial and portal vein smooth muscle cells by Ca(2+)-calmodulin-dependent kinase. *The Journal of Physiology*, *534*(Pt. 2), 395–408.

Greenwood, I. A., Ledoux, J., Sanguinetti, A., Perrino, B. A., & Leblanc, N. (2004). Calcineurin Aalpha but not Abeta augments ICl(Ca) in rabbit pulmonary artery

smooth muscle cells. *The Journal of Biological Chemistry*, *279*(37), 38830–7. http://doi.org/10.1074/jbc.M406234200

Harding, S. D., Sharman, J. L., Faccenda, E., Southan, C., Pawson, A. J., Ireland, S., … NC-IUPHAR. (2018). The IUPHAR/BPS Guide to PHARMACOLOGY in 2018: updates and expansion to encompass the new guide to IMMUNOPHARMACOLOGY. *Nucleic Acids Research*, *46*(D1), D1091–D1106. http://doi.org/10.1093/nar/gkx1121

Heinze, C., Seniuk, A., Sokolov, M. V, Huebner, A. K., Klementowicz, A. E., Szijártó, I. A., … Hübner, C. A. (2014). Disruption of vascular Ca2+-activated chloride currents lowers blood pressure. *The Journal of Clinical Investigation*, *124*(2), 675–86. http://doi.org/10.1172/JCI70025

Jensen, A. B., Joergensen, H. B., Dam, V. S., Kamaev, D., Boedtkjer, D., Füchtbauer, E.-M., … Matchkov, V. V. (2018). Variable Contribution of TMEM16A to Tone in Murine Arterial Vasculature. *Basic & Clinical Pharmacology & Toxicology*, *123*(1), 30–41. http://doi.org/10.1111/bcpt.12984

Li, R.-S., Wang, Y., Chen, H.-S., Jiang, F.-Y., Tu, Q., Li, W.-J., & Yin, R.-X. (2016). TMEM16A contributes to angiotensin II-induced cerebral vasoconstriction via the RhoA/ROCK signaling pathway. *Molecular Medicine Reports*, *13*(4), 3691–9. http://doi.org/10.3892/mmr.2016.4979

Manoury, B., Tamuleviciute, A., & Tammaro, P. (2010). TMEM16A/anoctamin 1 protein mediates calcium-activated chloride currents in pulmonary arterial smooth muscle cells. *The Journal of Physiology*, *588*(Pt 13), 2305–14. http://doi.org/10.1113/jphysiol.2010.189506

Mazzone, A., Bernard, C. E., Strege, P. R., Beyder, A., Galietta, L. J. V, Pasricha, P.

J., … Farrugia, G. (2011). Altered expression of Ano1 variants in human diabetic gastroparesis. *The Journal of Biological Chemistry*, *286*(15), 13393–403. http://doi.org/10.1074/jbc.M110.196089

Namkung, W., Phuan, P.-W., & Verkman, A. S. (2011). TMEM16A inhibitors reveal TMEM16A as a minor component of calcium-activated chloride channel conductance in airway and intestinal epithelial cells. *The Journal of Biological Chemistry*, *286*(3), 2365–74. http://doi.org/10.1074/jbc.M110.175109

Oh, S.-J., Hwang, S. J., Jung, J., Yu, K., Kim, J., Choi, J. Y., … Lee, C. J. (2013). MONNA, a potent and selective blocker for transmembrane protein with unknown function 16/anoctamin-1. *Molecular Pharmacology*, *84*(5), 726–35. http://doi.org/10.1124/mol.113.087502

Piper, A. S., & Greenwood, I. A. (2003). Anomalous effect of anthracene-9-carboxylic acid on calcium-activated chloride currents in rabbit pulmonary artery smooth muscle cells. *British Journal of Pharmacology*, *138*(1), 31–8. http://doi.org/10.1038/sj.bjp.0705000

Piper, A. S., & Large, W. A. (2003). Multiple conductance states of single Ca2+-activated Cl- channels in rabbit pulmonary artery smooth muscle cells. *The Journal of Physiology*, *547*(Pt 1), 181–96. http://doi.org/10.1113/jphysiol.2002.033688

Pritchard, H. A. T., Leblanc, N., Albert, A. P., & Greenwood, I. A. (2014). Inhibitory role of phosphatidylinositol 4,5-bisphosphate on TMEM16A-encoded calcium-activated chloride channels in rat pulmonary artery. *British Journal of Pharmacology*, *171*(18), 4311–21. http://doi.org/10.1111/bph.12778

Seo, Y., Lee, H. K., Park, J., Jeon, D.-K., Jo, S., Jo, M., & Namkung, W. (2016).

Ani9, A Novel Potent Small-Molecule ANO1 Inhibitor with Negligible Effect on ANO2. *PloS One*, *11*(5), e0155771. http://doi.org/10.1371/journal.pone.0155771

Shiffman, D., Rowland, C. M., Louie, J. Z., Luke, M. M., Bare, L. A., Bolonick, J. I., … Devlin, J. J. (2006). Gene Variants of VAMP8 and HNRPUL1 Are Associated With Early-Onset Myocardial Infarction. *Arteriosclerosis, Thrombosis, and Vascular Biology*, *26*(7), 1613–1618. http://doi.org/10.1161/01.ATV.0000226543.77214.e4

Sun, H., Xia, Y., Paudel, O., Yang, X.-R., & Sham, J. S. K. (2012). Chronic hypoxia-induced upregulation of Ca2+-activated Cl- channel in pulmonary arterial myocytes: a mechanism contributing to enhanced vasoreactivity. *The Journal of Physiology*, *590*(Pt 15), 3507–21. http://doi.org/10.1113/jphysiol.2012.232520

Thomas-Gatewood, C., Neeb, Z. P., Bulley, S., Adebiyi, A., Bannister, J. P., Leo, M. D., & Jaggar, J. H. (2011). TMEM16A channels generate Ca^{2+}-activated Cl^- currents in cerebral artery smooth muscle cells. *American Journal of Physiology. Heart and Circulatory Physiology*, *301*(5), H1819-27. http://doi.org/10.1152/ajpheart.00404.2011

Wang, B., Li, C., Huai, R., & Qu, Z. (2015). Overexpression of ANO1/TMEM16A, an arterial Ca2+-activated Cl− channel, contributes to spontaneous hypertension. *Journal of Molecular and Cellular Cardiology*, *82*, 22–32. http://doi.org/10.1016/j.yjmcc.2015.02.020

Wang, Q., Hogg, R. C., & Large, W. A. (1992). Properties of spontaneous inward currents recorded in smooth muscle cells isolated from the rabbit portal vein. *The Journal of Physiology*, *451*, 525–37.

Wei, L., Vankeerberghen, A., Cuppens, H., Eggermont, J., Cassiman, J. J.,

Droogmans, G., & Nilius, B. (1999). Interaction between calcium-activated chloride channels and the cystic fibrosis transmembrane conductance regulator. *Pflügers Archiv : European Journal of Physiology*, *438*(5), 635–41.

Wild, P. S., Felix, J. F., Schillert, A., Teumer, A., Chen, M.-H., Leening, M. J. G., … Dörr, M. (2017). Large-scale genome-wide analysis identifies genetic variants associated with cardiac structure and function. *Journal of Clinical Investigation*, *127*(5), 1798–1812. http://doi.org/10.1172/JCI84840

Wiwchar, M., Ayon, R., Greenwood, I., & Leblanc, N. (2009). Phosphorylation alters the pharmacology of Ca2+-activated Cl- channels in rabbit pulmonary arterial smooth muscle cells. *British Journal of Pharmacology*, *158*(5), 1356–1365. http://doi.org/10.1111/j.1476-5381.2009.00405.x

Yuan, X. J. (1997). Role of calcium-activated chloride current in regulating pulmonary vasomotor tone. *The American Journal of Physiology*, *272*(5 Pt 1), L959-68.

Table 1. Primer sequences used in qPCR experiments.

Gene	Forward Primers (+) (5'-3') Reverse Primers (-) (5'-3')	Gene ID	Amplicon size (base pairs)
TMEM16A	CCCTGTTCGTTGCGTCCTT	NM_001107564	121
	GCTCTGATGGCTACTGGTCTC		
Tmem16b	GGACGATGAGGATGATGAAGATAA	XM_017602863.1	128
	GATAGACAATGACCCCAAAGACA		
Myh11	CAGTTGGACACTATGTCAGGGAAA	XM_017596998.1	78
	ATGGAGACAAATGCTAATCAGCC		
Acta2	ATCCGATAGAACACGGCATC	NM_031004.2	228
	AGGCATAGAGGGACAGCACA		
Tnni3	TGACCTGCGTGGCAAGTT	NM_017144.2	153
	TCCTTCTCAATGTCCTCCTTCT		
Tnnt2	AGGAGGAAGGCTGAAGATGA	XM_006249842.3	126
	CTCTCGCTCTGTCTGTCTCT		
Pecam1	CTCCTAAGAGCAAAGAGCAACTTC	NM_031591.1	100
	TACACTGGTATTCCATGTCTCTGG		
Vwf	GTCGGAAGAGGAAGTGGACATT	NM_053889.1	136
	GGGCACACGCATGCGCTCTGTA		

Table 2. Cardiac parameters from Langendorff experiments. QT and RR intervals were extrapolated from ECG recorded by LabChart. Coronary flow was measured directly with ultrasonic flow meter probe. Data is expressed as mean±SEM, n=5-6. Paired t-test. *P < 0.05 from vehicle. #P < 0.05 from U46619.

Treatment	QT (ms)	RR interval (ms)	Coronary flow (ml/min)
Vehicle	64±9	174±20	9.9±0.1
$T16A_{inh}$-A01 (µM)			
0.01	62±7	168±19	9.9±0.1
0.03	65±9	179±21	10.2±0.1
0.1	73±8	174±21	10.2±0.2
0.3	72±8	166±22	11.1±0.3*
1	64±8	151±28	12.9±0.3*

Table 3. Cardiac parameters from Langendorff experiments. QT and RR intervals were extrapolated from ECG recorded by LabChart. Coronary flow was measured directly with ultrasonic flow meter probe. Data is expressed as mean±SEM, n=5. Paired t-test. *P < 0.05 from vehicle.

Treatment	QT (ms)	RR interval (ms)	Coronary flow (ml/min)
Vehicle	69±6	182±18	11.9±0.1
MONNA (µM)			
0.01	66±7	166±15	12.1±0.2
0.03	72±8	182±15	12.2±0.2
0.1	63±5	173±17	12.8±0.4
0.3	64±6	176±20	14.3±0.4*
1	74±8	191±20	20.7±1.0*
Vehicle	72±7	173±14	12.4±0.6
U46619 (µM)			
0.01	62±5	167±17	8.8±0.2*
MONNA + U46619 (µM)			
1.0 + 0.1	66±8	177±19	11.6±0.2#

Table 4. Mean EC_{50}s of U46619 and 5HT in coronary arteries from Wistar and spontaneously hypertensive rats in the presence and absence of different concentrations of the TMEM16A-specific inhibitor MONNA.

	DMSO	**1 μM MONNA**	**10 μM MONNA**
U46619 EC_{50} ±S.E.M (nM)			
NT	50.1±8	172.7±32	167.1±234
SHR	30.0±5	31.2±86	145.5±73
5HT(nM) (±S.E.M)			
NT	258.2±82	254.9±67	415.1±213
SHR	73.3±10	167.0±28	107.7±37

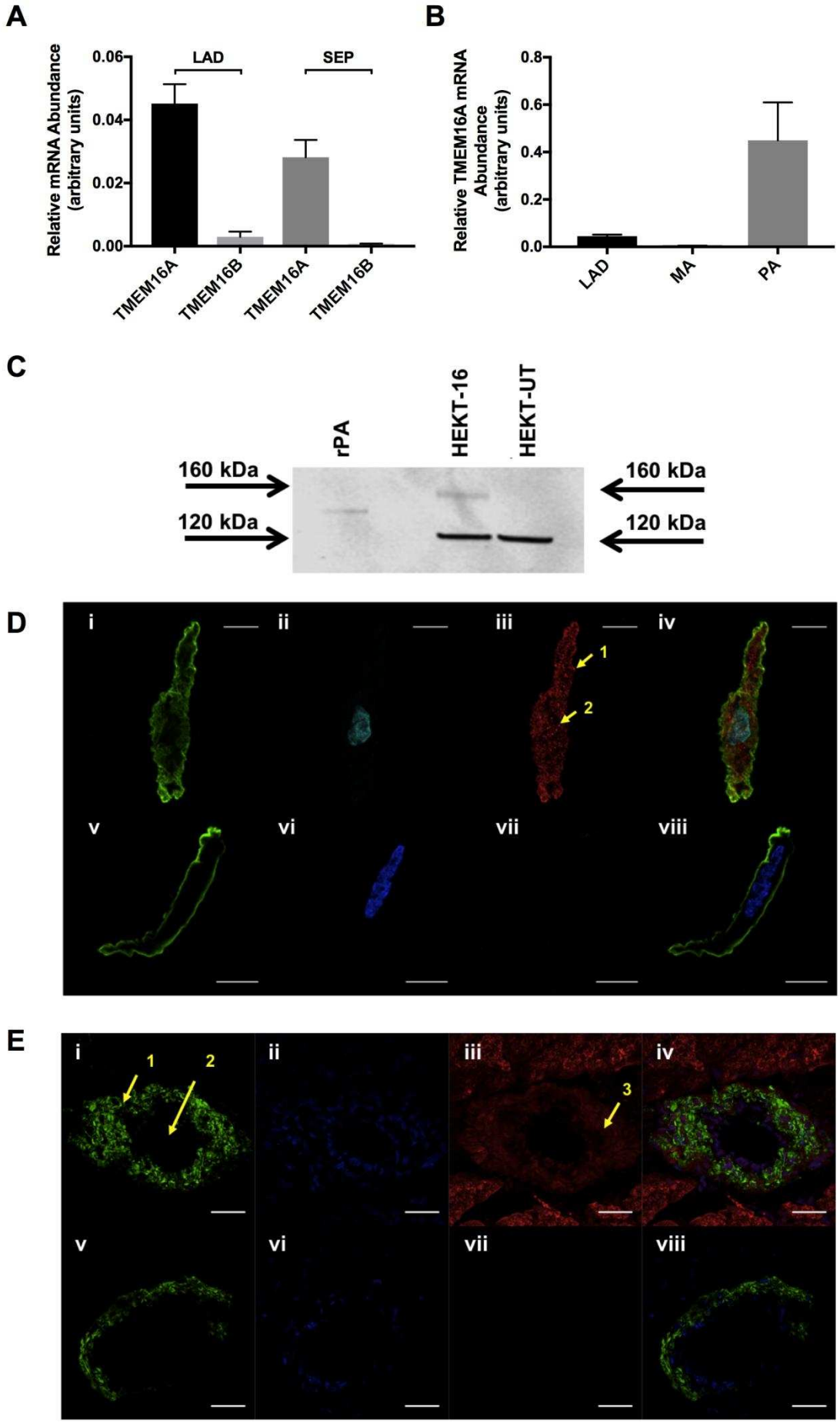

Figure 1. TMEM16A is expressed in rat coronary arteries. (A) Abundance of TMEM16A and TMEM16B mRNA relative to predetermined house-keeping genes in LAD and septal coronary arteries. n=3 where n is a pooled sample of arteries from at least 3 rats. (B) Abundance of TMEM16A mRNA relative to predetermined house-keeping genes in LAD coronary arteries, mesenteric arteries, and pulmonary arteries. n=3 where n is a pooled sample of arteries from at least 3 rats. (C) Western blot with anti-TMEM16A antibody AB53212 on lysates from rat pulmonary artery, TMEM16A-GFP-transfected HEK293 cells, and un-transfected HEK293 cells. Each rat sample constitutes 3 rats worth of tissue. (D) Single isolated VSMCs from LAD coronary arteries with anti-TMEM16A antibody AB53212 (i-iv). Cells are co-stained with anti-α smooth muscle actin (i and v), DAPI (ii and vi), anti-TMEM16A (iii), and a composite image (iv and viii). Arrows highlight small hotspots of intense staining. Images v-viii show a single VSMC isolated from a LAD coronary artery that was not incubated with an anti-TMEM16A primary antibody. Images are representative of at least 3 cells from arteries of 3 rats. Scale bar is 10 μm. (E) Images of a 16 μm thick slice of a rat where a coronary artery can be seen *in situ*, stained with anti-α smooth muscle actin (i and v), DAPI (ii and vi), +anti-TMEM16A (iii), -anti-TMEM16A (vii), and a composite image (iv and viii). Arrows 1 and 3 indicate the arterial wall within the myocardial tissue and arrow 2 highlights the lumen of the vessel. Images are representative of slices from 2 rats and 2-3 arteries per rat. Scale bar is 30 μm.

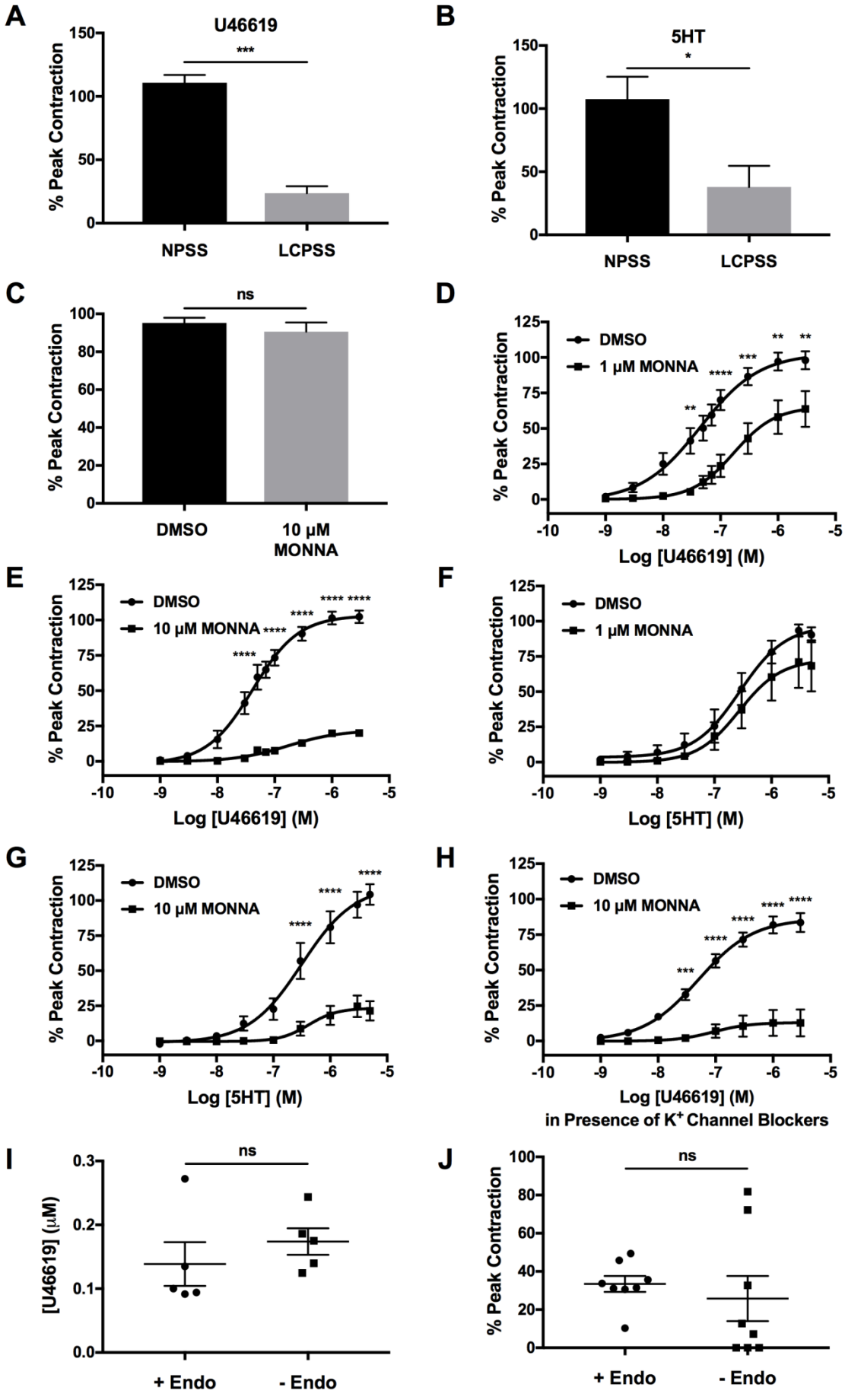

Figure 2. Inhibition of TMEM16A significantly attenuates coronary artery function. Bar charts showing that contractions of coronary arteries to U46619 (A) and 5HT (B) were significantly smaller when the segments were bathed in LCPSS; n=7 for U46619 and n=6 for 5HT. (C) Pre-incubation of 10 μmol/L MONNA had no effect on the KPSS-induced contraction in LADCA segments; n=6 for both DMSO and MONNA. (D) Pre-incubation with 1 μmol/L MONNA caused a significant attenuation of the U46619-induced response in LAD coronary arterials segments (n=8 for both DMSO and 1 μmol/L MONNA), while pre-incubation of 10 μmol/L MONNA significantly reduced the ability of the vessel to contract to U46619 (E) (n=8 for both DMSO and 10 μmol/L MONNA). (F) Pre-incubation with 1 μmol/L MONNA did not cause a significant attenuation of the 5HT-induced response in LAD coronary arterial segments (n=6 for both DMSO and 1 μmol/L MONNA), while pre-incubation of 10 μmol/L MONNA significantly reduced the ability of the vessel to contract to 5HT (G) (n=8 for both DMSO and 10 μmol/L MONNA). (H) Concentration-effect curves of U46619 in LADCA segments in the presence of K^+ channel blockers were significantly attenuated after incubation with 10 μmol/L MONNA; n=8 for both. (I) Scatter graph indicating that the EC_{50} of U46619 in LAD coronary artery segments in the presence of 10 μmol/L MONNA were similar in both endothelium intact, and denuded segments. Data are expressed as mean EC_{50} of U46619 ± S.E.M (in 10 μmol/L), n=5 for both. (J) The maximal contraction evoked by U46619 in LADCA segments incubated with 10 μmol/L MONNA was not different between endothelium intact and endothelium denuded segments; n=5 for both. All data are expressed as mean ± S.E.M. Statistical significance is defined as $P<0.05$ (*). ** indicates $P\leq0.01$, *** - $P\leq0.005$, **** - $P\leq0.001$.

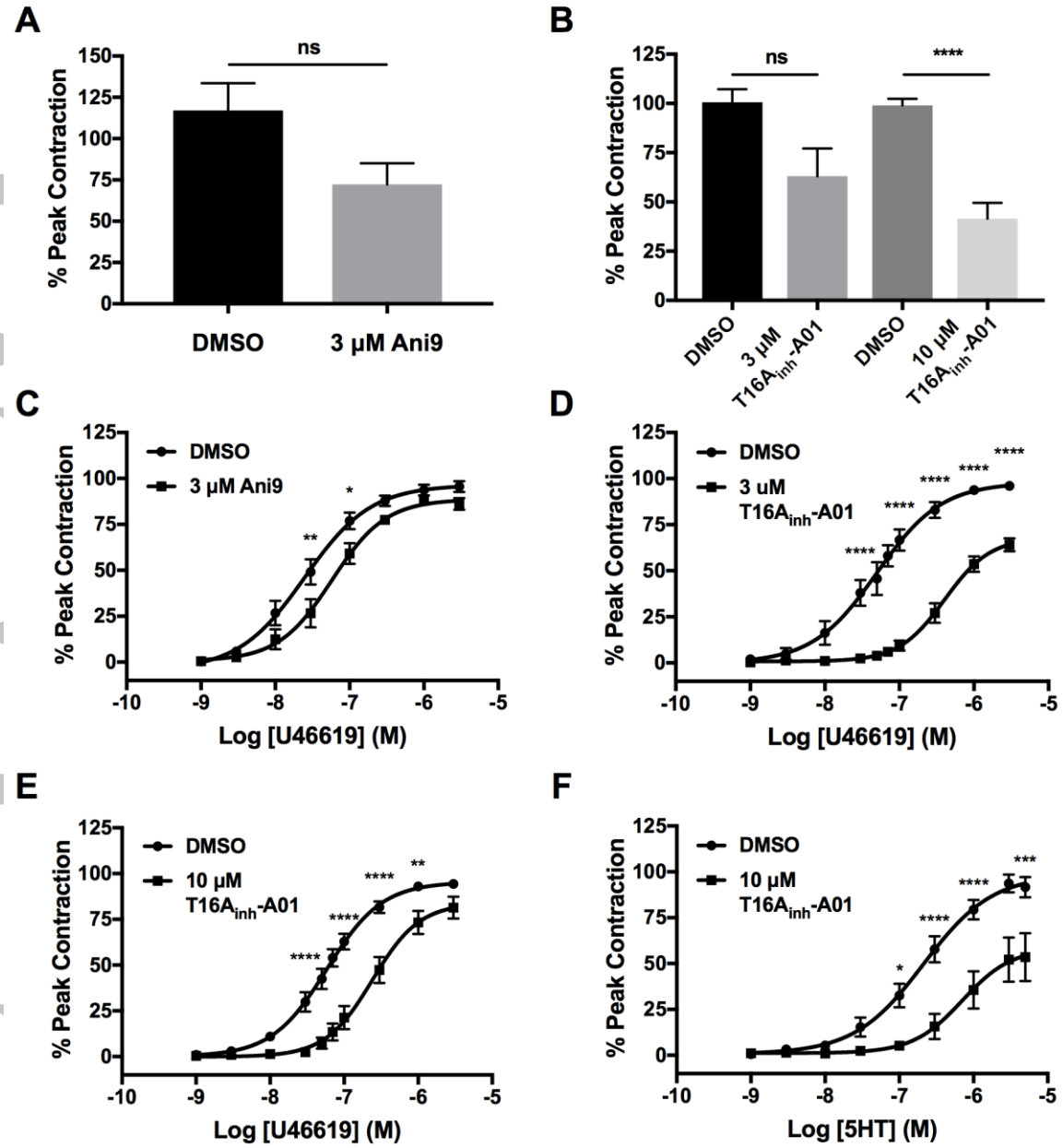

Figure 3. Effect of other TMEM16A inhibitors on coronary artery contractility. (A) Pre-incubation with 3 µmol/L Ani9 did not cause significant attenuation of the high K^+-induced contraction of coronary arteries (n=5 for both DMSO and 3 µmol/L Ani9). (B) While pre-incubation of 3 µmol/L $T16A_{inh}$-A01 did not cause a significant attenuation of high K^+-induced contraction of coronary arteries (n= 5 for both DMSO and 3 µmol/L $T16A_{inh}$-A01), pre-incubation with 10 µmol/L $T16A_{inh}$-A01 reduced the contractility considerably (n=12 for both DMSO and 10 µmol/L $T16A_{inh}$-A01). (C) U46619 concentration effect curves were significantly attenuated in the presence of

3 μmol/L Ani9 (n=6 for both DMSO and 3 μmol/L Ani9), 3 μmol/L T16A_{inh}-A01 (D) (n=9 for both DMSO and 3 μmol/L T16A_{inh}-A01), and 10 μmol/L T16A_{inh}-A01 (E) (n=10 for both DMSO and 10 μmol/L T16A_{inh}-A01). (F) 5HT concentration effect curves were also significantly impaired in the presence of 10 μmol/L T16A_{inh}-A01 (n=7 for both DMSO and 10 μmol/L T16A_{inh}-A01). All data are expressed as mean ± S.E.M. Statistical significance is defined as $P<0.05$ (*). ** indicates $P\leq0.01$, *** - $P\leq0.005$, **** - $P\leq0.001$.

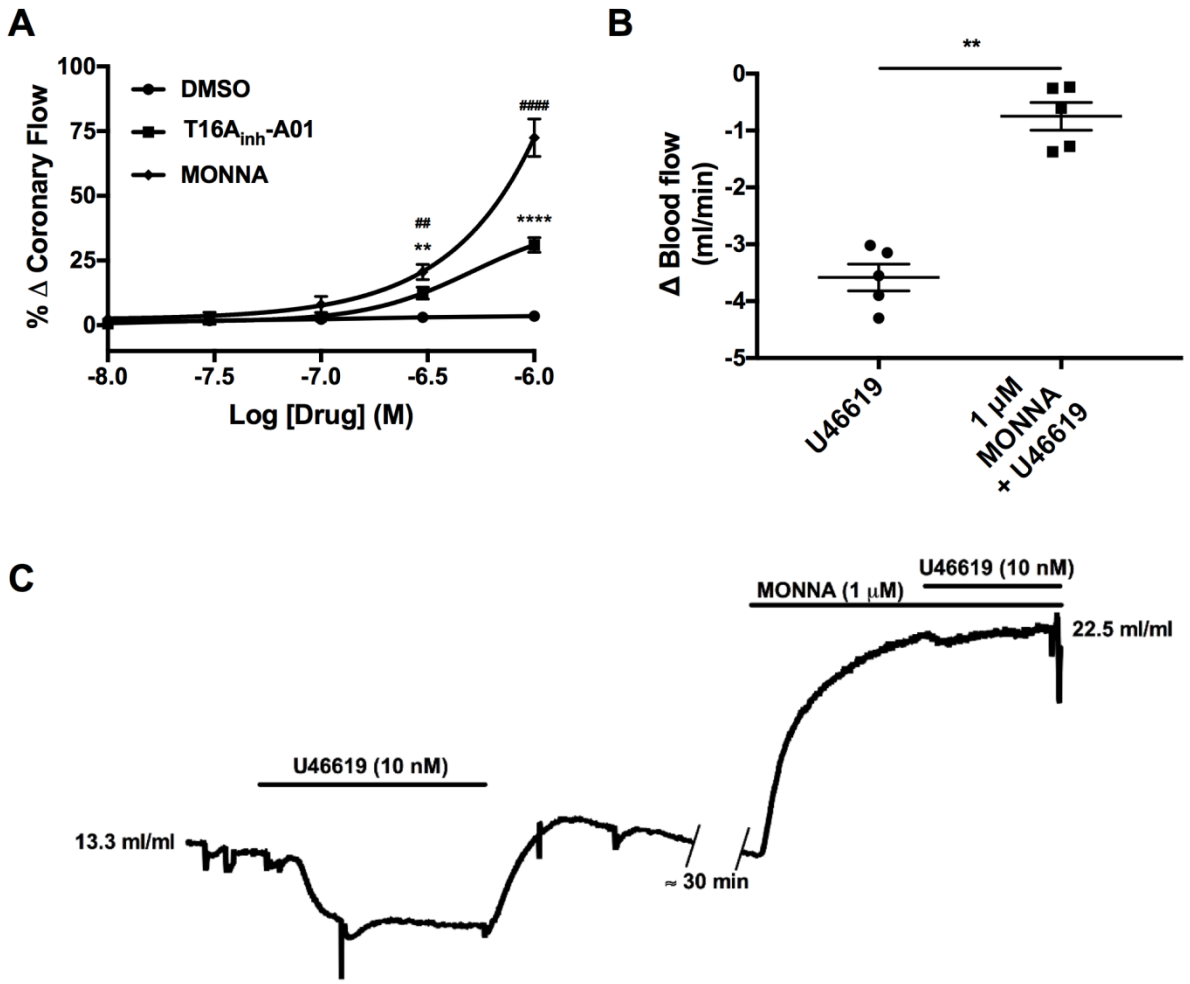

Figure 4. Inhibition of TMEM16A significantly increases coronary flow. (A) Application of MONNA and T16A$_{inh}$-A01 caused a concentration-dependent increase in coronary flow (n=6 for MONNA, n=5 for T16A$_{inh}$-A01, and n=5 for DMSO). Pre-incubation with 1 μmol/L MONNA prevented U46619-induced reductions in coronary flow (B) (n=5 for both conditions). C shows a representative trace from the experiment described in B. All data are expressed as mean ± S.E.M. Statistical significance is defined as $P<0.05$ (*). ** indicates $P\leq0.01$, *** - $P\leq0.005$, **** - $P\leq0.001$.

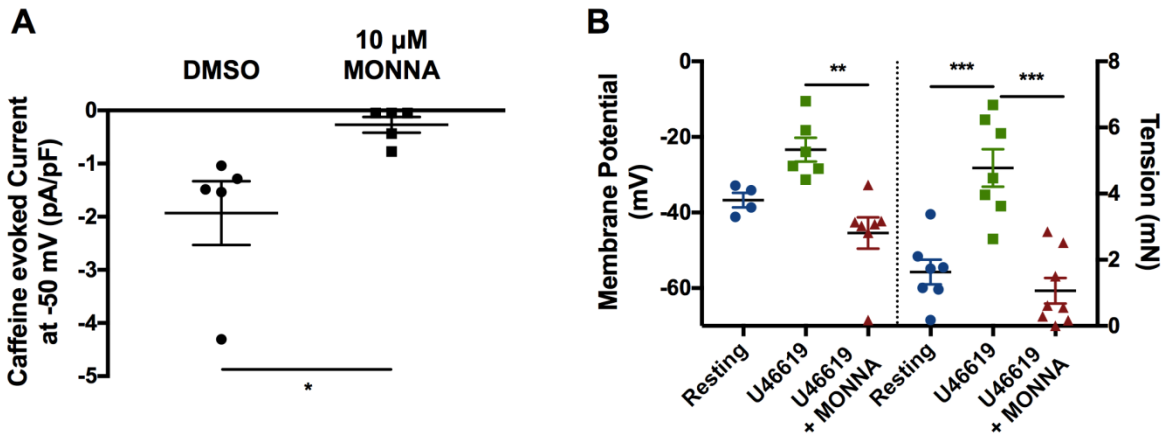

Figure 5. The scatter plot shows the increase in current evoked from LAD coronary artery VSMCs, at a holding potential of -50 mV, upon application of 10 mmol/L Caffeine in the absence and presence of 10 µmol/L MONNA; n=5. Scatter graph showing the membrane potential (left, mV), and evoked contraction (right, mN) in resting, +U46619, and +U46619+10 µmol/L MONNA; n=4 for resting E_M, n=6 for E_M in U46619, and n=7 for E_M in U46619+10 µmol/L MONNA, and n=7 for tension recordings in resting and U46619, and n=8 in U46619+10 µmol/L MONNA. All data are expressed as mean ± S.E.M. Statistical significance is defined as $P<0.05$ (*). ** indicates $P\leq0.01$, *** - $P\leq0.005$, **** - $P\leq0.001$.

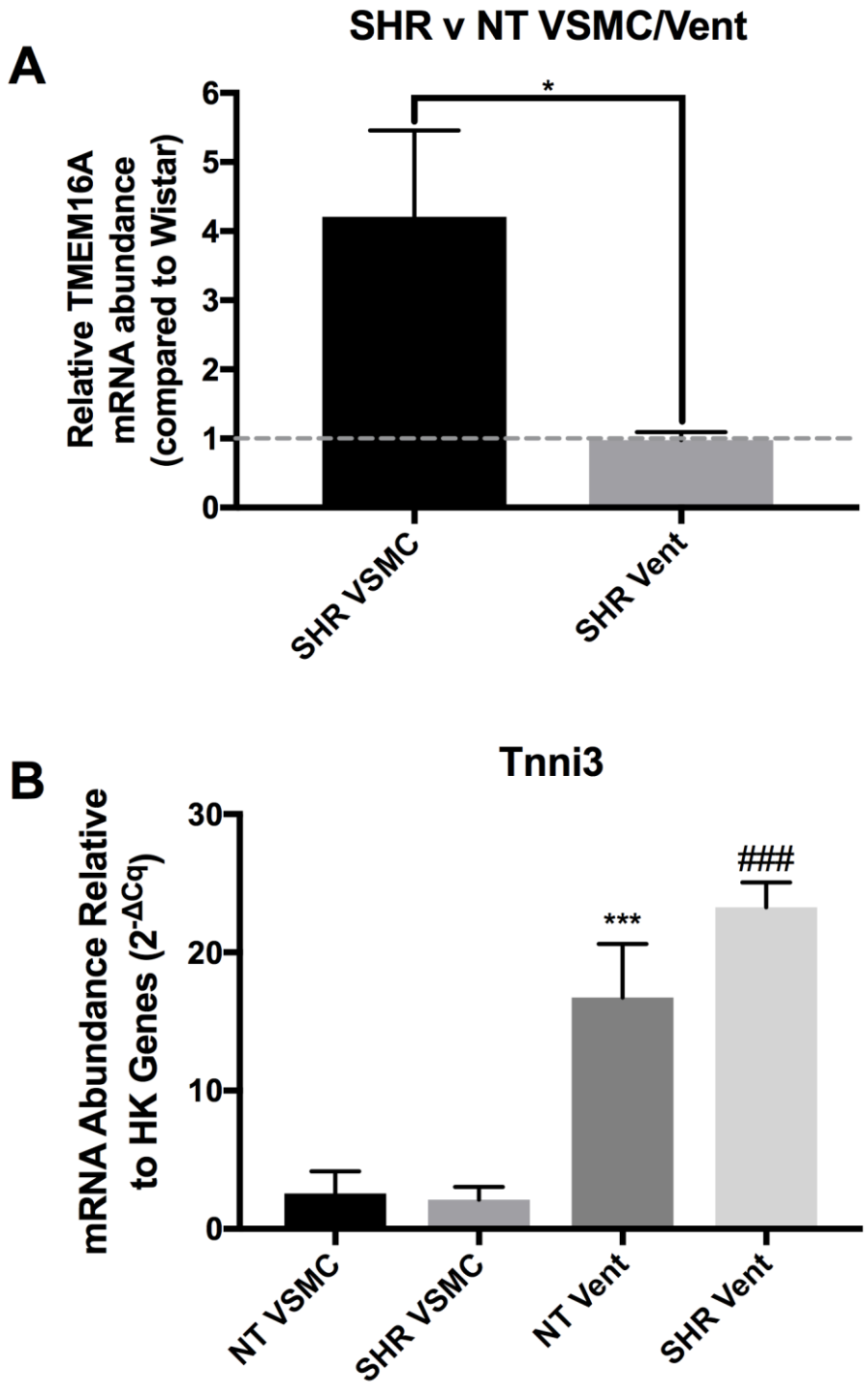

Figure 6. Increased expression of TMEM16A in coronary arteries from spontaneously hypertensive rats. (A) TMEM16A mRNA is expressed at levels approximately four-fold greater in coronary arteries SMCs from SHRs when compared to Wistar rats. There was no increase in TMEM16A expression in the ventricular tissue from SHRs. (B) The expression of the cardiac-specific marker

troponin I3 (Tnni3), was expressed at negligible levels in the coronary artery SMC samples of both Wistar rats and SHRs, and expression was significantly greater in the ventricular tissue of the same rats (* for Wistar tissues, # for SHR tissues). All data are expressed as mean ± S.E.M of at least 5 separate rat samples. Statistical significance is defined as $P<0.05$ (*). ** indicates $P\leq0.01$, *** - $P\leq0.005$, **** - $P\leq0.001$.

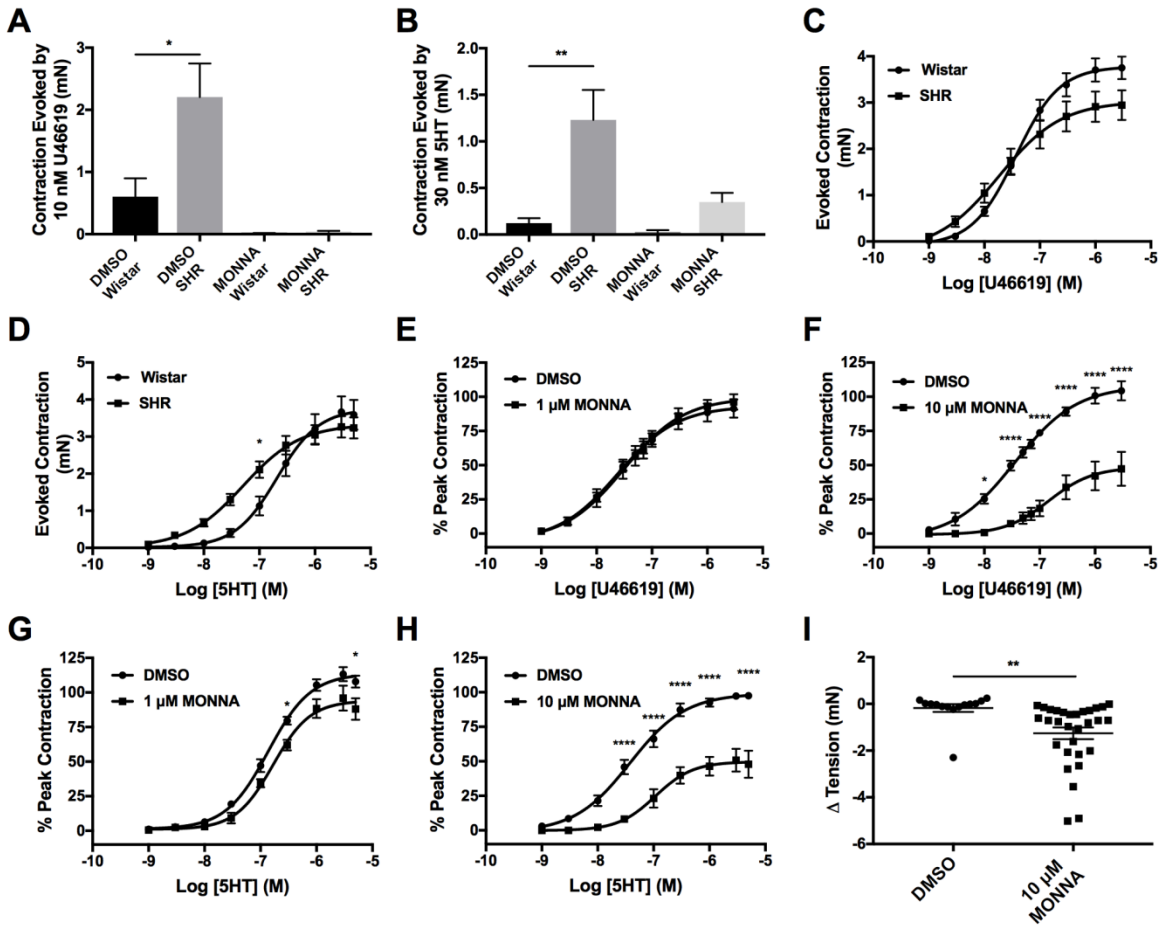

Figure 7. Altered function of TMEM16A in LAD coronary arteries from spontaneously hypertensive rats. (A) Increases in contractility of LAD coronary arteries from SHRS in response to lower concentrations of U46619 (n=8 for Wistar and n=6 for SHRs) and 5HT (B) (n=9 for Wistars and n=7 for SHRs) were abolished by pre-incubation with 10 µmol/L MONNA. LAD coronary arteries from SHRs were more sensitive to constriction with U46619 (n=27 for Wistar and n=16 for SHR) and 5HT (n=12 for Wistar and n=13 in SHRs) (C and D). (E) Pre-incubation with 1 µmol/L MONNA has no effect on the U46619 concentration-effect curve in LAD coronary artery segments of SHRs. (F) Pre-incubation with 10 µmol/L MONNA significantly attenuates the ability of the vessel to constrict to U46619. (G) Pre-incubation with 1 µmol/L MONNA has a small but significant effect on the 5HT concentration-effect curve in LAD coronary artery segments of SHRs. (H) Pre-incubation with 10 µmol/L MONNA

significantly attenuates the ability of the vessel to constrict to 5HT. (I) Basal tone developed in LAD coronary artery segments of SHRs was significantly suppressed by application of 10 μmol/L MONNA. All data are expressed as mean ± S.E.M. Statistical significance is defined as $P<0.05$ (*). ** indicates $P\leq0.01$, *** - $P\leq0.005$, **** - $P\leq0.001$.